Noise in Distributed Raman Amplification

Philippe Gallion[a], JunHe Zhou[a,b], ShiFeng Jiang[a], JianPing Chen[b], and Yves Jaouën[a]
[a]Ecole Nationale Supérieure des Télécommunications,
GET, Télécom Paris et CNRS, LTCI UMR 5141
46, rue Barrault, 75634 Paris Cedex 13, France
Phone: (+33) 1 45 81 77 02, Fax: (+33) 1 45 89 00 20, Email: philippe.gallion@enst.fr
[b]SKL of AOCSN, Shanghai Jiao Tong University,
800 Dongchuan Rd Shanghai 200240, P. R. China

ABSTRACT

Fundamental noise limitations of distributed quantum amplifiers are discussed. For Raman amplifier pumps to signals noise transfer, Rayleigh backscattering and polarization fluctuations of the pump are additional noise sources, which are discussed including their impact on system performances.

Keywords:
Quantum noise, noise figure Raman amplifier, noise transfer, Rayleigh backscattering, polarization fluctuations, optical system performances.

1 INTRODUCTION

Because their optical gain per unit of length is small, most of the optical amplifiers work as Traveling Wave Amplifier (TWA) over a propagation length significantly large as compared to the optical wavelength. Distributed Raman Fiber Amplifiers (DRFA) based on the Stimulated Raman Scattering (SRS) are well-known to offer the advantages to provide a flat gain and a wideband amplification in conventional low-loss silica fibers itself, at any wavelength for which a pump, with frequency higher than that of signal by the Stokes shift, is available[1,2]. They also allow a distributed amplification over length of several tens of km which is significantly larger than the distribution length of Erbium Doped Fiber Amplifiers (EDFA)[3], just acting as nearly lump amplifiers when they are used in long span transmission. Therefore DRFA allows smaller magnitude excursion of the signal level and therefore low non-linearity impairments and lower noise than EDFA amplifiers.

To take advantage of these potentialities, noise properties analysis is a key issue in DRFA design and analysis. The 3 first major noise sources are the Fundamental Quantum Noise (FQN) generation[4,5], usually expressed in terms of Amplified Spontaneous Emission (ASE), corrected by output shot noise ad hoc addition[6,7,8], the pump-to-signal noise transfer, and the Double Raleigh Backward Scattering (DRBS)[9]. We will point out that the random birefringence, well-known to be at the origin of the Polarization Mode Dispersion (PMD), also induces pumping noise transfer and acts as fourth source of noise.

Because of the simultaneous amplification of the two non commutating quadratures of the optical field, any phase insensitive linear amplifier is subject to intrinsic quantum noise generation well known to lead to the 3 dB noise figure minimum, in the high gain limit[10,5]. In section 2, we will first consider this intrinsic noise generation and show that it is produced by the amplification of vacuum fluctuation input noise and by the intrinsic quantum amplification and attenuation noises mechanisms. Because of the very fast relaxation of the optical phonon, the lower state of pumped DRFA is nearly empty and the virtual inversion population is almost complete, keeping the quantum noise very close to its minimum value. Fundamental limits for the noise of homogeneous gain distribution over a lossy fiber will be discussed[11]. Results will be compared to those of the standard ASE beating noise description. Performance of DRFA as usually compared to lumped Erbium Doped Fiber Amplifier (EDFA). The better noise performances of the former are usually expressed by the so-called effective noise figure. However, since this concept may be misleading because the so-

Passive Components and Fiber-based Devices IV,
edited by Ming-Jun Li, Jianping Chen, Satoki Kawanishi, Ian Hugh White,
Proc. of SPIE Vol. 6781, 67810U, (2007) · 0277-786X/07/$18 · doi: 10.1117/12.741561

called effective noise figure could be negative we discuss the relation between standard and effective noise figure definitions.

We will first briefly recall the basics of Raman amplification[2] in section 3 and precise its fundamental noise mechanism and ultimate noise figure limit. As stimulated Raman scattering is nearly independent of the pump and signal propagation direction, fiber Raman amplifiers can work both for the counter propagating and co propagating pump with respect to the signal. These 2 configurations have different and contradictory interests with respect to intrinsic noise generation and to pump noise transfer[12].

The second noise impairment, discussed in section 4, is the pump noise transfer[13]. It results from the fact that the small Raman absorption cross-section requiring high power pumps exhibiting usually a large noise, described in terms of Relative Intensity Noise (RIN). Because Raman amplification operates through virtual excited states, no population inversion smoothes out the pumps fluctuations, and an instantaneous value of the signal experiments through propagation a fluctuating value of the gain, resulting of short time averaging over the pump to signal walk-off time. Since a large gain is first experimented, propagation of the signal and the pump is in the same direction is preferable, as far as only intrinsic noise is concerned. On the other hand, counter propagation configuration is more favorable when pump-to-signal noise transfer is concerned, because the cut-off frequency of intensity noise transfer from the pump to the signal is lower. Since multi pump amplification is required to achieve an flat and wide optical bandwidth compatible with Wavelength Division Multiplexing (WDM) application, we proposed a novel frequency model to evaluate the pump to signal intensity noise transfer in multi pump amplification of multiple WDM signals. The model takes into account the pump depletion and pump-to-pump, pump-to-signal and signal-to-signal interaction.

The Rayleigh scattering in the optical media is due to the random fluctuations of the refractive index on a scale much smaller than the optical wavelengths[1], leading to optical scattering loss that has a wavelength dependence of λ^{-4}. In the common silica-based single-mode fibers (SMF), the Rayleigh scattering loss is typically around 0.12-0.16 dB/km at 1.55μm [1]. In addition to causing the optical loss in SMF, Rayleigh scattering also reflects a fraction of the incident mode into the contra-propagating one, resulting in the phenomenon of Double Rayleigh Backscattering (DBR). In section 5 we will discuss the influence of DBR in terms of system penalty by taking into account its polarization degree with respect to that of the output signal.

We will finally pointed out, in section 6, that the pump State of Polarization (SOP) temporal fluctuations in the presence of PMD influence the amplified signal noise and propose an analytical expression of the transfer function and cutoff frequency[14]. Influence, in terms of Q penalty, will be discussed.

2 FUNDAMENTAL QUANTUM NOISE IN DISTRIBUTED AMPLIFICATION

2.1 Localized linear phase insensitive linear optical amplification

Let us consider an optical ideal phase insensitive and linear amplifier. The input to output transfer relation for the two optical field quadrature operators X and Y would be in this case, in the form[15]

$$\begin{pmatrix} X \\ Y \end{pmatrix}_{OUT} = \begin{pmatrix} \sqrt{G} & 0 \\ 0 & \sqrt{G} \end{pmatrix} \begin{pmatrix} X \\ Y \end{pmatrix}_{IN} \tag{2.1}$$

where G is the optical power gain. In this case we would have the average commutator relationship

$$\left\langle \left[X_{OUT} Y_{OUT} \right] \right\rangle = G \left\langle \left[X_{IN} Y_{IN} \right] \right\rangle \tag{2.2}$$

where $[\ ]$ stands for the operator commutator $\left[\hat{X}\hat{Y}\right] = \hat{X}\hat{Y} - \hat{Y}\hat{X}$ and $\langle\ \rangle$ stands for the ensemble averaging. So the input to output transformation does preserve the commutator (obviously except for G =1) and this transformation is not canonical in the Hamiltonian meaning. Heisenberg uncertainty product is directly linked to commutator by

$$\left\langle \Delta X^2 \right\rangle^{1/2} . \left\langle \Delta Y^2 \right\rangle^{1/2} = \delta X \ \delta Y \ \geq \frac{1}{2} \left| \left\langle \left[XY \right] \right\rangle \right| = \frac{h\nu}{2} B_0 \tag{2.3}$$

where B_O is the optical bandwidth and $h\nu$ the photon energy. Such an input to output relation does not preserve input Heisenberg uncertainty principle[10]. So, the input to output relation must mandatory include an additional noise contribution N_X and N_Y and be in the form

$$\begin{pmatrix} X \\ Y \end{pmatrix}_{OUT} = \begin{pmatrix} \sqrt{G} & 0 \\ 0 & \sqrt{G} \end{pmatrix} \begin{pmatrix} X \\ Y \end{pmatrix}_{IN} + \begin{pmatrix} N_X \\ N_Y \end{pmatrix} \tag{2.4}$$

The output commutator is then written as

$$\langle [X_{OUT} Y_{OUT}] \rangle = G \langle [X_{IN} Y_{IN}] \rangle + \langle [N_X N_Y] \rangle + \sqrt{G} \langle [X_{IN} N_Y] \rangle + \sqrt{G} \langle [N_X Y_{IN}] \rangle \tag{2.5}$$

where the last 2 terms vanish out since signal and noise are independent.
The preservation of commutator allows us to calculate the average minimum required additional noise contribution commutator which is

$$\langle [N_X N_Y] \rangle = (1-G) \langle [X_{IN} Y_{IN}] \rangle \tag{2.6}$$

For a singe polarization and an optical bandwidth B_O, the corresponding the added noise power P_A is found to be

$$P_A = \delta X \delta Y = |1-G| \frac{h\nu}{2} B_0 \tag{2.7}$$

This result is in good agreement with the standard Amplified Spontaneous Emission (ASE) average power derivation. This noise contribution is independent of the amplification of the input noise and is to be added to the additional noise free contribution derived from Eq.2.2. By adding second order momentum we obtain the minimum uncertainty product

$$\delta X_{OUT} \delta Y_{OUT} = [G + |1-G|] \frac{1}{2} \langle [X_{IN} Y_{IN}] \rangle \tag{2.8}$$

For large values of the gain *G,* these two added noise contributions are close, meaning that, in the large gain limit, the minimum value of noise figure of the amplifier is 2, i.e. 3dB. This result is valid for any type of linear phase insensitive amplifier.
For the particular case of a laser amplifier, the total output noise is the Amplified Spontaneous Emission (ASE), which in fact consists of an amplification of the incoming vacuum fluctuations and the contribution of carrier momentum fluctuation at the optical frequency. The latter provide the mandatory additional noise and the minimum value of the noise figure is only obtained when a perfectly population inverted medium is assumed.

2.2 Noise figure for distributed amplifiers

The standard approach of fundamental noise of a laser amplifier is usually performed in term of ASE and the associated beat noise[6,7]. It has been shown that a more general and more accurate description may be performed in terms of amplification of the vacuum fluctuation input noise and of the intrinsic amplification and attenuation noises mechanisms[15,16].

Let us consider the optical power spectral density of zero-point field fluctuations with the single-sided optical power spectral density of noise as the fundamental input noise[17,18,19]

$$S_{N0} = h\nu / 2 \tag{2.9}$$

Despite its dependence on the optical frequency, the optical power spectral density is considered as an Additive Gaussian White Noise (AGWN), in the narrow optical band approximation. Its is to be mentioned that, as the thermal noise in the radiofrequency range, the zero-point field fluctuation noise level do not depends of the signal level and it is to be considered as the minimum input noise in optical amplifier noise analysis, even when no other input signal is applied.
As well known in the radiofrequency range, a noise generation is also associated, in the optical domain, to any attenuation or beam partition process, due to fluctuation-dissipation theorem. For the light amplification through an elementary slice of width *dz* in a medium with the gain per unit of length β, the elementary noise contribution required to fulfill the commutator conservation is a differential version of Eq 2.7 for the single sided power spectrum and expressed as

$$dS = \beta \frac{h\nu}{2} dz \tag{2.10}$$

Considering an absorption coefficient per unit of length α, the elementary noise contribution to the single sided power spectrum is expressed as

$$dS = \alpha(h\nu/2)dz \tag{2.11}$$

Let us consider now a slice of width *dz* of an amplifier medium with both a gain per unit of length β and a attenuation per unit of length α. The single-sided spectral density $S_N(\omega,z)$ of optical noise is found to follow the propagation equation

$$dS_N = \underbrace{(\beta-\alpha)S_N dz}_{\text{Noise Amplification}} + \underbrace{\left[(\beta+\alpha)(h\nu/2)dz\right]}_{\text{Noise Generation}} \tag{2.12}$$

In the general case the gain the coefficient β decays, due to pump absorption and pump depletion and the general solution of Eq.2.12 is expressed as incomplete gamma functions. Under assumptions of an amplification *L* shorter than the effective length corresponding to pump absorption and depletion, the gain as well as the loss do not depend of the coordinate, the general solution of Eq.2.12 is reduced to

$$S_N(z) = C\exp(\beta-\alpha)z - \frac{\beta+\alpha}{\beta-\alpha} h\nu/2 \tag{2.13}$$

C is an integration constant. Assuming an input noise spectral density $S_N(0)$, the total output noise spectral density for an overall amplification length *L* is found to be

$$S_N(L) = K(G-1)(h\nu/2) + GS_N(0) \tag{2.14}$$

G is the net gain defined as $G = \exp(\beta-\alpha)L$ and *K* the multiplicative noise excess factor as compared to the minimum added amplification noise $(G-1)h\nu/2$, required to fulfill minimum uncertainty product requirement. *K* in expressed as

$$K = (\alpha+\beta)/|\beta-\alpha|. \tag{2.15}$$

Using the definition of signal to noise ratio and noise figure *F* in the optical domain[20,21] and making reference to a coherent state input, i.e. vacuum fluctuations, input noise $S_N(0) = h\nu/2$, the total output of Fundamental Quantum Noise (FQN) noise is expressed as

$$S_N(L) = FG(h\nu/2) \tag{2.16}$$

Using the standard definition, and making reference to vacuum fluctuation input level, the Noise Factor *F*, denoted Noise Figure (NF) when expressed in dB, is expressed as:

$$F = K\frac{(G-1)}{G} + 1 \approx K + 1 \quad \text{for} \quad G >> 1 \tag{2.17}$$

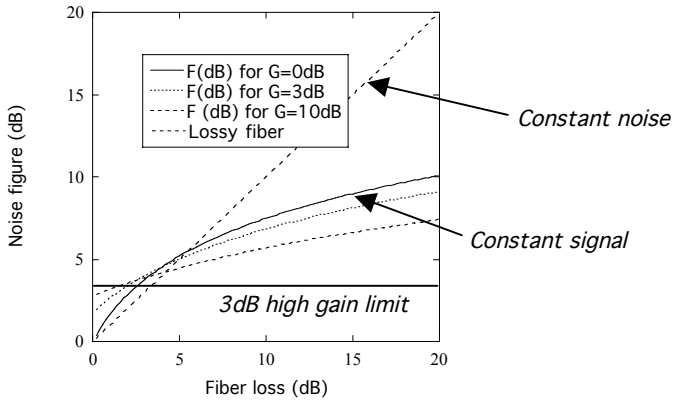

Figure 3.1: Noise figure as a function of fiber loss for various values of the net gain

Introducing the built in internal loss attenuation $A = \exp(-\alpha L)$, the noise figure given by Eq.2.17 can be also expressed as

$$F = \frac{\ln G - 2\ln A}{\ln G}\frac{G-1}{G} + 1 \tag{2.18}$$

The noise figure, for various values of the achieved net gain and as a function of fiber loss, is shown on Figure 3.1. The noise figure is obviously found to be less than the "3db limit" for the low values of the built in loss and of the achieved net gain[13]. For a purely attenuating medium with $\beta = 0$, implying $G = A$, the signal propagation is at a constant level, and the noise figure is $F = 2\alpha L + 1$. For an exact and local attenuation and gain compensation $\beta = \alpha$ implying an overall gain $G=1$, the noise figure is $F = 1/A$. Noise figure tends to the 3dB high gain limit when the overall gain increase making noise enhancement by the built in loss is negligible. It is to be noticed that the optical noise figure concept is only relevant when the input noise in specified and when it is defined in the optical domain and for unsaturated amplifier for which the gain is independent of the signal and for which no noise regression occurs.

2.3 Comparison with the Amplified Spontaneous Emission approach

It is interesting to compare the general result given by Eq 2.16 and 2.17, which do not required the specification of the physical phenomena in charge of the FQN generation, to the well-know particular situation of laser amplification in which FQN generation is usually expressed in terms of Amplified Spontaneous Emission (ASE). The output average ASE power is usually obtained by considering that, according to the basic Einstein's laser rate equation, the average spontaneous emission in a single mode corresponds to 1 photon. Considering again a gain coefficient β and attenuation α, the spectral density on spontaneous emission S_{ASE} is governed by the equation

$$dS_{ASE} = \underbrace{(\beta-\alpha)S_{ASE}dz}_{\text{Spontaneous Emission Amplification}} + \underbrace{\beta h\nu dz}_{\text{Spontaneous Emission Generation}} \tag{2.19}$$

It is to be noticed that the amplification is proportional to the net gain (β - α), while the spontaneous emission generation is only governed by the total gain β. By solving this equation in the ideal homogeneous case where gain and loss coefficient do not depend of the coordinate and assuming that the there is no input noise we obtain the total output ASE

$$S_{ASE}(L) = n_{SP}(G-1)h\nu \quad \text{with} \quad n_{SP} = \beta/(\beta-\alpha) \tag{2.20}$$

n_{SP} is well known to be the inversion population factor (sometime called the spontaneous emission enhancement factor). Eq.2.19 is well known to be incomplete for the total output noise description and the shot noise of the output signal contribution is to be added. This can be performed by adding $h\nu/2$ to equation Eq.2.20, which is afterward and finally found equivalent to Eq.2.14 because we have $2n_{SP} = K + 1$.

Despite it finally allows us to find the good result, the weakness of the ASE model is to only calculate the average ASE power and to require photodetection and associated beat noise to take into account its stochastic nature. One may, of course, also wonder why only phase noise is taken into account in beat noise description and why no amplitude fluctuations are associated to ASE at this level. The ASE model does not consider the quantum noisy nature of light as an input noise, misses the quantum nature of light as an output noise and needs an heuristic ad hoc correction to take it into account. Furthermore, the concept of inversion population factor n_{SP} for a Raman amplifier, in which this inversion is only virtual, is at least misleading. It is to be noticed that the spectral density of quantum noise in simply obtained by adding half of the photon energy to the spectral density on spontaneous emission.

$$S_{N\pm}(z,\omega) = S_{ASE\pm}(z,\omega) + \frac{h\nu}{2} \tag{2.21}$$

2.4 Equivalent lumped amplifier noise figure

Performances of a distributed amplifier is usually expressed in terms of the noise figure F_{LUMP}, for a hypothetic lumped amplifier, localized after the corresponding attenuating section, and producing the same amount of ASE power. Observing that the noise figure F_{FIBER} of a pure attenuation fiber is related to its attenuation coefficient by $F_{FIBER} = 1/A$ and using the standard cascading noise figure formula, this noise figure is expressed as $F_{LUMP} = AF$. This value is strongly dependent on the attenuation of the fiber and may be obviously less than the 3dB ($F = 2$) high gain limit of an ideal amplifier for which $K = n_{SP} = 1$. This equivalent noise figure may be of course also negative, when expressed in dB.

3 BASICS OF RAMAN AMPLIFICATION

The principle of Raman amplification is the scattering of a photon, at the pump wavelength, with energy transferred to a photon at the signal wavelength and a phonon absorbed by the silica of the fiber[1,2]. SRS may transfer down the energy from the pump by subtraction of the phonon frequency of $\Omega/2\pi$ =13,2 Thz, for GeO_2 Silica fiber, to the pump frequency (Raman Stokes), or up, by the same photon frequency addition to the pump frequency (Raman anti Stokes). The two types of transition exist, with the probabilities respectively proportional to $(1+n_q)$ and n_q, where $n_q = \left(\exp(\hbar\Omega/kT)-1\right)^{-1}$ is the Bose-Einstein phonon population number. This phonon population number is 0.13 at T = 300 K and for optical frequencies in the low attenuation window. As the stimulated Stokes Raman scattering is usually the amplifying process, the anti Stokes diffusion acts an attenuation source.

In a DRFA, due to the pump attenuation and to the pumps depletion by the signal, the amplification gain per unit of length β and an attenuation per unit of length α change along the propagation according to

$$\beta(z) = \left(1+n_q\right)C_R P_P(z) \text{ and } \alpha(z) = \alpha_S + n_q C_R P_P(z) \tag{3.1}$$

$P_p(z)$ is the pump power, α_S is the total attenuation coefficient at he signal frequency and C_R is the Raman gain coefficient at the given signal and pump frequencies. The Raman gain coefficient C_R is defined as

$$C_R = \frac{g_R}{2A_{eff}} \tag{3.2}$$

A_{eff} is the mode effective area, taking into account pump confinement and pump with signal overlap, and the factor 2 is the reduction of the co-polarization Raman efficiency g_R, since the Raman efficiency of the pump component with a polarization orthogonal with the signal is negligible.

The net gain coefficient governing the energy transfer from the pump to the signal and therefore the net local gain is expressed as

$$\beta(z) - \alpha(z) = C_R P_P(z) - \alpha_S \tag{3.3}$$

Assuming that a perfect distribution of gain can be achieved the fundamental noise factor of Raman, in the high gain limit is written as

$$F_{MinRaman} = 2\left(1+n_q\right) \approx 2.26 \text{ i.e. } 3.5dB \tag{3.4}$$

This value is impossible to achieved due to pump absorption and signal depletion and the main goal of pump engineering is to approach it. The pumping schemes for Raman amplification includes the forward pumping, the backward pumping and the bidirectional pumping. The power evolutions of a depolarized pump P_P and a signal P_S traveling in a fiber are described by the basic equations

$$\pm\frac{dP_P}{dz} = -\frac{\nu_P}{\nu_S}C_R P_S P_P - \alpha_P P_P \quad \text{and} \quad \frac{dP_S}{dz} = +C_R P_S P_P - \alpha_S P_S \tag{3.5}$$

The sign ± stands for the co propagation and counter propagation of the pump. ν_P is the pump frequency, ν_S the signal frequency, α_P is the attenuation coefficient at the pump frequency.

Forward pumping scheme, in which the pump and the signal co-propagate in the optical fiber, first seems more interesting for the noise optimization and was studied at first. However, experiments have rapidly demonstrated a strong intensity noise transfers from the pump to signal in this configuration. Since the group velocity difference between the pump and signal is small, the intensity noise on pump is only averaged over a very short time and is easily transferred to the signal degrading the system performances. In the backward pumping scheme, the signal and the pump propagate in the counter direction, and hence the walk-off effect between the pump and signal time averages the fluctuations of the pump value experimented by the signal and prevents the high frequency noise component transfer from the pump to the signal. For these reasons, backward pumping has received more attention later on. Furthermore counter-propagating is more robust to gain saturation resulting of the pump depletion. However, with the advance in the low noise laser diode technology, more attention is now paid on the co propagating pumping configuration. If the RIN level is roughly less than -110dB/Hz, co-directional pumping can be employed to have better noise performance of the Raman amplifiers. The bidirectional multi pumping can balance the noise figure to flatten the noise level within the gain spectrum and its

optimization is another key issue in Raman fiber amplifiers. By using multiple pumps, one is able to obtain a flattened gain spectrum within 100nm. The nonlinearity of coupled equation prevents the linear optimization methods from application in WDM systems

4 PUMP TO SIGNAL INTENSITY NOISE TRANSFER

We have proposed a novel frequency model to evaluate the pump to signal intensity noise transfer in multi pump amplification, including a large number of pumps to achieve homogeneous properties over a wide frequency range, and for WDM signals including a large number of channels[22,23]. The model takes into account the pump depletion and pump-to-pump, pump-to-signal and signal-to-signal interaction as well.

$$\pm\frac{dP_i}{dz}=\sum_{i,j\#i}^{m+n} g(\nu_i,\nu_j)P_iP_j-\alpha_iP_i \tag{4.1}$$

Where the sign + indicates forward propagation, the sign – indicates backward propagation. n is the number of signal channels of the WDM multiplex, *m* is the number of pumps. P_i and P_j are the powers of the *i*th and *j*th pump or signal wave propagating along the fiber, respectively. $g(\nu_i,\nu_j)$ is the Raman gain coefficient between frequency ν_i and frequency ν_j.

Before introducing the frequency model, we make the assumption that the amplitude of the pump fluctuation $\Delta P_i(z,t)$ is relatively small as compared to the steady state pump power $P_i(z)$ and satisfies the coupled equation Eq 4.1, in which we have omitted the second order term

$$\pm\frac{\partial\Delta P_i(z,t)}{\partial z}+\frac{1}{v_{g,i}}\frac{\partial\Delta P_i(z,t)}{\partial t}=\sum_{j=1,j\neq i}^{n+m} g(\nu_i,\nu_j)P_i(z)\Delta P_j(z,t)+\sum_{j=1,j\neq i}^{n+m} g(\nu_i,\nu_j)P_j(z)\Delta P_i(z,t)-\alpha_i\Delta P_i(z,t) \tag{4.2}$$

Taking Fourier transform on Eq. (4.2) and rewriting it in matrix form, one has:

$$\frac{\partial\Delta P(z,\omega)}{\partial z}=A\Delta P(z,\omega)\quad\text{with}\quad\Delta P(z,\omega)=\begin{pmatrix}\Delta P_1(z,\omega)\\ \vdots\\ \Delta P_m(z,\omega)\end{pmatrix} \tag{4.3}$$

and A is a matrix with corresponding elements. The general solution have the following form

$$\Delta P(L,\omega)=M_{RIN}\Delta P(0,\omega)\quad\text{with}\quad M_{RIN}=\lim_{\Delta z\to 0}\prod_{k=1}^{L/\Delta z}\left(I+A(k\Delta z)\Delta z\right) \tag{4.4}$$

I is the identity matrix and M_{RIN} can be evaluated numerically via a forward Euler method, a Runge-Kutta method or a Picard method. For the co-pumped RFAs, $\Delta P(0,\omega)$ is known and the RIN transfer $\Delta P_s(L,\omega)$ can be simply calculated by multiplying the matrix. For the counter-pumping scheme, the RIN transfer can also be evaluated. We achieve this by separating the vector $\Delta P(0,\omega)$ into $\begin{bmatrix}\Delta P_p(0,\omega)\\ \Delta P_s(0,\omega)\end{bmatrix}$, $\Delta P(L,\omega)$ into $\begin{bmatrix}\Delta P_p(L,\omega)\\ \Delta P_s(L,\omega)\end{bmatrix}$ and the matrix M_{RIN} into $\begin{pmatrix}M_{11} & M_{12}\\ M_{21} & M_{22}\end{pmatrix}$ respectively. Since the intensity noise on the signal at the input end of the fiber is zero, $\Delta P_S(0,\omega)=0$, therefore the Eq.4.4 becomes:

$$\begin{pmatrix}\Delta P_{p\_out}\\ \Delta P_{s\_out}\end{pmatrix}=\begin{pmatrix}M_{11} & M_{12}\\ M_{21} & M_{22}\end{pmatrix}\begin{pmatrix}\Delta P_{p\_in}\\ 0\end{pmatrix} \tag{4.5}$$

and the signal intensity noise at the output end is

$$\Delta P_{p\_out}=M_{21}M_{11}^{-1}\Delta P_{p\_out} \tag{4.6}$$

For sake of simplification it has been proven[23], for the single pump and single signal case, that our model can derive the exactly the same formula as in Ref.13. Now we are going to consider the results for the multiple pump case.

Considering, a standard single mode fiber with the length of 50km is used as the gain media. The second order dispersion coefficient β_2 and the third order dispersion coefficient β_3 are -20.41 ps^2/km and 0.1734 ps^3/km at the wavelength of 1550nm. 80 channels of signals are launched into the fiber with 100GHz channel spacing. The input signal power for each channel is –10dbm. Different pumping schemes are investigated upon this length of fiber sharing the same pumping wavelength, i.e. 1425nm, 1440nm, 1450nm, 1465nm and 1490nm. The gain profile for the co-pumping scheme has been equalized and the corresponding pump powers are 440.8mW, 312.9mW, 116.7mW, 180mW, and 39.1mW. The maximum gain ripple is 0.9dB.

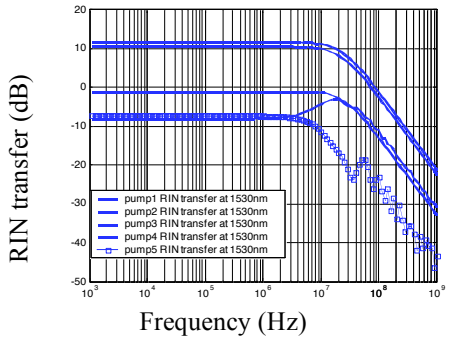

Fig. 4.1: Intensity noise transfer of the co-pumped 50km RFA at 1530nm

In Fig. 4.1, the intensity noise transfers from the pumps to the signal channels at the wavelength of 1530nm is demonstrated. Different pump induce different intensity noise transfer on the signal channels. Pump 1 causes the most significant intensity noise transfer. One more interesting phenomenon is that the intensity noise transfer from pump 4 to the signal channel at 1530nm reaches maximum at the frequency of about 200MHz. This has not been observed in single pump case. It may be caused by the complex coupling between the pumps and the signals, which transfers the intensity noise from pump 4 to pump 3.

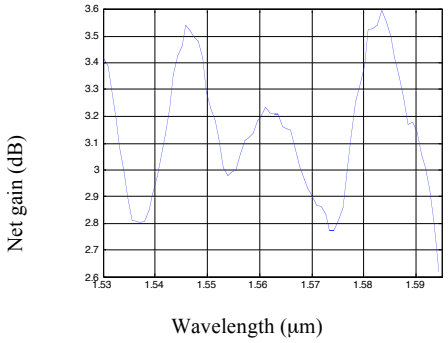

Fig. 4.2. Net gain spectrum of the counter-pumped 50km RFA

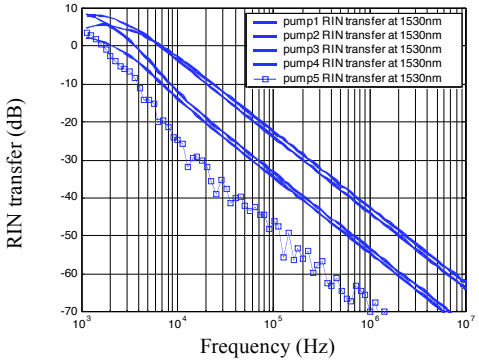

Fig. 4.3. Intensity noise transfer of the counter-pumped 50km RFA at 1530nm

For the counter-pumping scheme, the Raman gain spectrum is illustrated in Fig. 4.2. The gain profile has also been equalized and the corresponding pump powers are 397.1mW, 288.2mW, 111.4mW, 180.1mW, and 47.4mW. The maximum gain ripple is about 1dB.

The intensity noise transfer from pump 1 to pump 5 to the signal channel at 1530nm is plotted in Fig. 4.3. Similarly, it can also be inferred that in counter-pumping scheme the pump providing more gain on the signal will cause more intensity noise transfer.

5 IMPACTS OF RAYLEIGH BACKSCATTERING

5.1 Model of noise propagation and the noise properties in the presence of Rayleigh backscattering

Rayleigh backscattering is due delta-correlated fluctuations of the propagation constant inside the fiber, resulting in the linear coupling between the for- and backward traveling modes in SMF. Rayleigh backscattering is characterized by a differential coupling constant γ_R, called Rayleigh backscattering coefficient. With the quasi-monochromatic approximation, and taking into account the Rayleigh backscattering and the generation of the intrinsic noise in the two directions, we can model the spatial evolution of the forward and backward optical power spectral densities of noise in a DRFA by the following equation

$$\pm\frac{\partial}{\partial z}S_{N\pm}(z,\omega)=g(z)S_{N\pm}(z,\omega)+\gamma_R S_{N\mp}(z,\omega)+\left[\left(1+2n_q\right)C_R P_P(z)+(\alpha_S-\gamma_R)\right]h\nu \tag{5.1}$$

where $S_{N\pm}(z,\omega)$ are the forward and backward spectral densities of noise and $h\nu$ is the energy of a signal photon. It is to be noticed that γ_R is to be subtracted from loss noise generation, since it corresponds to power coupling of the 2 counter propagating modes. The solving of Eq.5.1) is in fact a boundary value problem that can be solved numerically. It can be generalized by taking into account the frequency dependence of all the parameters and the depletion of the Raman pumps [24]. For high Raman gains, i.e., $G_R > 30$ dB, because of the Rayleigh backscattering, the pump saturation is enhanced by the multiple reflections and amplification of the signal and the total ASE. When the pump saturation is negligible, the first effect of the Rayleigh backscattering on the DRFA-based transmission systems are the amplified single backscattering of the backward traveling ASE leading to noise figure degradation. Due to the linear nature of Eq 5, it can be seen that the DRB noise should have a spectrum identical to that of the signal and the second DRB effect is an important in-band crosstalk induced by the amplified DRB of the signal. It has been shown that the signal and the DRB noise are practically uncorrelated in time[25,26], which means that, at the receiver, the signal beats not only with ASE but also with the DRB noise as well.

The associated noise fields to DRB and ASE can be both considered as circular complex Gaussian random variables[25,26], but the former is colored whereas the later is nearly white. Apart from this, it is also well known that, different from the unpolarized ASE noise, the DRB noise has the same state of polarization as the output signal and its degree of polarization is 1/9 of that of the output signal [27]. In the notation of Jones vectors, we can write the output field of a DRFA as: $|A_s\rangle = A_L|e_s\rangle + |A_N\rangle$, where A_L and $|e_s\rangle$ are the slowly varying envelope and the unitary Jones vector (2D column complex) of the amplified signal, and $|A_N\rangle = |A_{DRB}\rangle + |A_{ASE}\rangle$ is the total noise field. We assume that the amplified signal is fully polarized, which means $|e_s\rangle$ does not vary with time. It is usual to describe the polarization properties of a quasi monochromatic light in terms of a coherence matrix whose elements are the self and cross correlation function of the transverse components of the field

$$J=\begin{pmatrix}R_{xx}(\tau) & R_{xy}(\tau)\\ R_{yx}(\tau) & R_{yy}(\tau)\end{pmatrix} \quad \text{where} \quad R_{xy}(\tau)=E\left[A_x(t+\tau)A_y^*(t)\right] \tag{5.2}$$

$E[\ ]$ stands for the statistical average. The diagonal terms are the intensities corresponding to the 2 axis and the trace of $\boldsymbol{J}$ is the total intensity for $\tau = 0$.

Therefore, if choosing $|e_s\rangle$ as the one of the two principle axes, say, x-axis, the coherence matrix of the total noise field is diagonal since the noise on the 2 polarizations are independent. Therefore we have

$$\mathrm{E}\left[\left|A_N(t+\tau)\right\rangle\left\langle A_N(t)\right|\right]=\begin{bmatrix}R_x(\tau) & 0\\ 0 & R_y(\tau)\end{bmatrix}=S_{ASE}\begin{bmatrix}1 & 0\\ 0 & 1\end{bmatrix}\delta(\tau)+K_R\begin{bmatrix}5/9 & 0\\ 0 & 4/9\end{bmatrix}R_L(\tau) \tag{5.3}$$

where S_{ASE} is the optical power spectral density of the ASE noise on one polarization, and

$$K_R=\gamma_R^2\int_0^L\int_0^z G^2(z)/G^2(x)\,\mathrm{d}x\mathrm{d}z \tag{5.4}$$

is the DRB crosstalk coefficient, with $G(z)=\exp\int_0^z g(x)\,\mathrm{d}x$ being the amplifier gain[28,29].

5.2 The *Q*-factor penalty due to Rayleigh backscattering

For calculating the exact bit-error rate of the systems employing DRFA with Rayleigh backscattering, we have developed a semi-analytical method[23]. For simplification, however, we will only present here an analysis of the *Q*-factor penalty due to Rayleigh backscattering. Assuming that the beating noise dominates, the *Q*-factor can be found as [25,29]

$$Q\approx\frac{\iint_{\Re^2}X_L(t-\tau_1)K(\tau_1,\tau_2)X_L^*(t-\tau_2)\,\mathrm{d}\tau_1\mathrm{d}\tau_2}{\sqrt{2\iint_{\Re^4}X_L(t-\tau_1)K(\tau_1,\tau_2)R_x(\tau_2-\tau_3)K(\tau_3,\tau_4)X_L^*(t-\tau_4)\,\mathrm{d}\tau_1\mathrm{d}\tau_2\mathrm{d}\tau_3\mathrm{d}\tau_4}} \tag{5.5}$$

with the integral kernel given by

$$K(\tau_1,\tau_2)=\int_{\Re}H_o(\tau_1-\tau_3)H_e(\tau_3)H_o(\tau_2-\tau_3)d\tau_3 \tag{5.6}$$

where H_o and H_e are the optical and electrical filters before and after the photodiode, and X_L is the optical field pulse-shape of "1"s. The *Q*-factor penalty due to Rayleigh backscattering is defined, here, as the ratio of the *Q*-factors without, Q_0, and with Rayleigh backscattering, Q_R. From (4.3) and (4.6), it can be found, in decibels, as

$$\Delta Q\,(\mathrm{dB}Q)=10\log_{10}\left(\frac{Q_0}{Q_R}\right)=5\log_{10}\left(1+\Delta\eta_{ASE}+\frac{10}{9}\Delta\eta_D K_R Q_0^2\right) \tag{5.7}$$

where $\Delta\eta_{ASE}=S_{ASE}/S_{ASE,0}-1$ is the ASE enhancement factor that we define as the normalized difference between the ASE spectral densities with and without Rayleigh backscattering, and, assuming the simple backscattering of the backward ASE dominates, it can be found from (4.1) as

$$\Delta\eta_{ASE}\approx\gamma_R\int_0^L\int_0^z\frac{G(z)P_p(z)}{G^2(x)}\mathrm{d}x\mathrm{d}z\Big/\int_0^L\frac{P_p(z)}{G(z)}\mathrm{d}z\,; \tag{5.8}$$

and the constant $\Delta\eta_D$, depending uniquely on the modulation format and the detection configuration, is given by

$$\Delta\eta_D=\frac{\iint_{\Re^4}X_L(t-\tau_1)K(\tau_1,\tau_2)R_L(\tau_2-\tau_3)K(\tau_3,\tau_4)X_L^*(t-\tau_4)\,\mathrm{d}\tau_1\mathrm{d}\tau_2\mathrm{d}\tau_3\mathrm{d}\tau_4}{\left[\iint_{\Re^2}X_L(t-\tau_1)K(\tau_1,\tau_2)X_L^*(t-\tau_2)\,\mathrm{d}\tau_1\mathrm{d}\tau_2\right]^2}. \tag{5.9}$$

For example, in a direct-detection system using 40 Gbit/s RZ format, where the signal power pulse shape is Gaussian with a full width half maximum (FWHM) temporal width of 6.25ps (1/4 bit duration), the optical filter is Lorentzian with a 3-dB bandwidth of 0.4 nm ($f_{3\mathrm{dB}}$ = 50GHz) and the electrical filter is a 2nd order Butterworth filter with $f_{3\mathrm{dB}}$ = 30GHz, we have $\Delta\eta_D$ = 0.2 at the maximum point of the output pulse of the electronic circuit.

In the figure 5.1, we have plotted the DRB crosstalk coefficient, the ASE enhancement factor and the Q penalty as a function of the percentage of forward pumping and the Raman gain in a 100 km long bidirectionally-pumped DFRA. As seen in figure 5.1(a) and (b), the DRB crosstalk coefficient and the ASE enhancement factor increase both much more

rapidly with the Raman gain as in unidirectionally-pumped DFRA than in a bidirectionally-pumped DFRA. Moreover, we see that the DRB crosstalk is symmetric with respect to the 50% forward pumping, whereas the ASE enhancement is not and is found to be less in forward pumping than in backward. Figure 5.1(c) shows clearly that the bi-directional pumping with forward pumping around 50%-60% is very interesting for its tolerance on the penalty due to Rayleigh scattering.

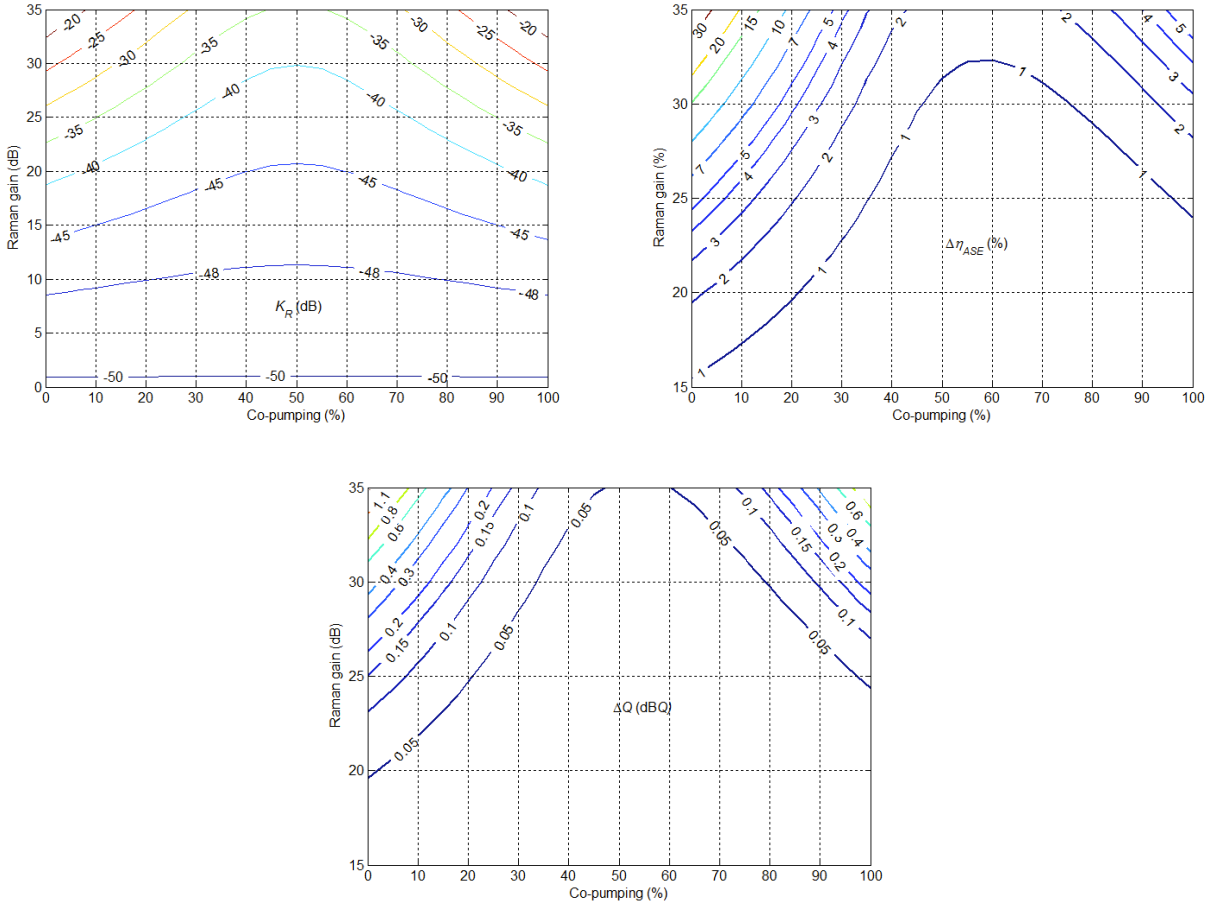

Fig. 5.1 Examples of (a) the DRB crosstalk coefficient, (b) the ASE enhancement factor and (c) the Q penalty as a function of the percentage of the forward pumping and the Raman gain in a 100 km long bidirectionally-pumped DFRA. Parameters: $\lambda_{s/p}$ = 1455 / 1555 nm, $\gamma_R = 1\times10^{-7}$ km^{-1}, $\alpha_{s/p}$ = 0.20 / 0.26 dB/km, C_R = 0.69 W^{-1}km^{-1} and $\Delta\eta_D$ = 0.2.

6 PMD ASSISTED PUMP TO SIGNAL NOISE TRANSFER

In the section 4, we have discussed the impact of the pump to signal noise transfer. However, it was in fact based on a scalar description of the SRS process, where the Raman pumps should be depolarized. It is well known that the SRS process is polarization dependent. As the Raman pumps are polarized, the PMD due to the birefringence of the optical fibers can lead to the Raman gain fluctuations and the polarization dependent gain[30]. Although the depolarization of the Raman pumps can compensate these impairments, we have shown that additional noises can be induced to the signal because of the pump SOP temporal fluctuations associated with the PMD[31].

6.1 Model of signal propagation taking into account the polarization effects

Taking into account the polarization dependence of SRS, and working in a frame of reference traveling with the pump, we can write the signal propagation equation as[14,30]

$$\frac{\partial P_s}{\partial z}+\beta_{sp}\frac{\partial P_s}{\partial t}=\left[C_R P_p\left(1+\vec{s}_s\cdot\vec{s}_p\right)-\alpha_s\right]P_s \tag{6.1}$$

where $\beta_{sp}=v_s^{-1}\mp v_p^{-1}$ is the pump signal walk-off parameter, $\vec{s}_s$ and $\vec{s}_p$ are the SOP Stokes vectors of the signal and the pump, that are 3D column unitary vectors, defined on the Poincaré sphere[30]. Moreover, we add another rotating frame in such a manner that the pump SOP is not affected by the fiber birefringence[30]. Now, to simplify the following analysis, we assume that the pump SOP does not change with the length of the fiber in the two frames of reference, i.e., $\vec{s}_p=\vec{s}_p(t)$. Neglecting the impact of pump on the signal SOP, and assuming the latter is fixed at the input, we have[14,30]

$$\frac{d}{dz}\vec{s}_s=\vec{b}_{sp}\times\vec{s}_s,\ \text{with}\ \vec{b}_{sp}=\left(1\mp\frac{\nu_P}{\nu_S}\right)\mathbf{R}^{-1}\vec{\beta}_s, \tag{6.2}$$

where $\mathbf{R}$ is a 3D rotation matrix governed by $\mp d/dz(\mathbf{R})=\eta_{ps}=(\nu_P/\nu_S)\vec{\beta}_s\times\mathbf{R}$, with $\mathbf{R}(0)=\mathbf{I}$, and $\vec{\beta}_s$ is the local birefringence vector at the signal frequency[30], that we describe using the model proposed in Ref.33 and experimentally validated[32]. With this model, we have shown that the autocorrelation matrix of the signal SOP is given by[14]

$$\left\langle\vec{s}_s(z)\vec{s}_s^{\mathrm{T}}(z+u)\right\rangle=\frac{\mathbf{I}}{3}C_{ss}(u)=\frac{\mathbf{I}}{3}C_{ss}(-u),\ \text{for}\ z>>L_d, \tag{6.3}$$

where L_d is the diffusion length defined as $L_d=\int_{u\geq 0}C_{ss}(u)\,\mathrm{d}u$, and C_{ss} is the scalar autocorrelation function. After an elaborated analysis, we have shown that this scalar function can be found numerically by using a set of recursive equations. For co-pumping, we have shown it can be approximated by the analytical expression proposed in Ref.30: $C_{ss}(u)=\exp\left(-|u|/L_d\right)$, where $L_d=6\pi D_p^{-2}(\nu_P-\nu_S)^{-2}$ with D_p being the PMD parameter[33]. For counter-pumping, however, the numerical simulation is generally necessary.

6.2 Analysis on the SOP fluctuations induced signal noises

We assume the pump is depolarized, which means $\mathrm{E}[\vec{s}_p(t)]=\vec{0}$. However, because of its definition, the pump SOP vector is always instantaneously unitary and, therefore, rotates randomly in time on the Poincaré sphere. Moreover, because of the PMD, the signal SOP rotates randomly, in the rotating frame, relative to the pump SOP with the length of the fiber. Therefore, from (6.1) where the signal amplification depends on the inner product of these two SOP vectors, i.e., $\vec{s}_s\cdot\vec{s}_p=\vec{s}_s(z)\cdot\vec{s}_p(t)$, we see that their random fluctuations can obviously induce noises to the signal. To analyze the noise transfer, we write the signal and pump powers as $P_\mu=\overline{P}_\mu\left(1+m_\mu\right)$, where m_s and m_p are the signal and pump modulation indexes representing the noises, and $\overline{P}_s(z,t)$ and $\overline{P}_p(z)$ are the transmitted powers without noises. Then from Eq.6.1, we can find in the first order

$$\frac{\partial m_s}{\partial z}+\beta_{sp}\frac{\partial m_s}{\partial t}=C_R\overline{P}_p\left(m_p+m_{sp}\right),\ \text{with}\ m_{sp}(z,t)=\vec{s}_s(z)\cdot\vec{s}_p(t). \tag{6.4}$$

Since the RIN is just the spectral density of the modulation index, i.e., $\mathrm{RIN}(f)=\mathbf{TF}\left[\ \mathbf{E}\left[m(t+\tau)m(t)\right]\ \right]$, Eq.6.4 shows clearly that, apart from the pump to signal RIN transfer discussed in the section 4, the RIN of the amplified signal results also from the pump SOP fluctuations.

It is useful to define the pump SOP spectral density as $S_{\mathrm{SOP}}(f)=\mathbf{TF}\left[\ \mathbf{E}[\vec{s}_p(t+\tau)\cdot\vec{s}_p(t)]\ \right]$. Since the pump intensity fluctuations are generally small, we can find with approximation, for depolarized pumps,

$$S_{\mathrm{SOP}}(f)\approx\mathrm{RIN}_p(f)+S_{xy}(f),\ \text{with}\ S_{xy}(f)=2\overline{P}_p^{-2}\mathbf{TF}\left[\left\langle A_x^*(\tau)A_x(0)A_y(\tau)A_y^*(0)+A_x(\tau)A_x^*(0)A_y^*(\tau)A_y(0)\right\rangle\right] \tag{6.5}$$

where $\mathrm{RIN}_p(f)$ is the RIN of the pump, and $A_{x,y}$ are the field envelopes the two pump polarization components. In what follow, we will call $S_{xy}(f)$ as the relative beating spectrum. Then, by solving Eq.6.4, we can find the PMD averaged signal RIN at the output as[14]

$$\left\langle\mathrm{RIN}_s(f)\right\rangle=\left|\underline{h}_{\mathrm{RIN}}(L,f)\right|^2\mathrm{RIN}_p(f)+\left|\underline{H}_{\mathrm{SOP}}(f)\right|^2S_{\mathrm{SOP}}(f)=\left|\underline{H}_{\mathrm{RIN}}(L,f)\right|^2\mathrm{RIN}_p(f)+\left|\underline{H}_{\mathrm{SOP}}(f)\right|^2S_{xy}(f), \tag{6.6}$$

where $\left|\underline{h}_{\mathrm{RIN}}(L,f)\right|^2$ is just the traditional RIN transfer function[13],

$$\left|\underline{H}_{\mathrm{SOP}}(L,f)\right|^2 \approx \frac{1}{3}C_R^2 P_{p0}^2 L_{eff}\,\mathbf{TF}\left[C_{ss}\right]\left(2\pi\beta_{sp}f\right),\ \text{with}\ L_{eff}=\int_0^L P_p^2(z)\,\mathrm{d}z/P_{p0}^2 \tag{6.7}$$

will be called as the SOP fluctuations transfer function, and $\left|\underline{H}_{\mathrm{RIN}}(L,f)\right|^2=\left|\underline{h}_{\mathrm{RIN}}(L,f)\right|^2+\left|\underline{H}_{\mathrm{SOP}}(L,f)\right|^2$ is, therefore, the novel pump to signal RIN transfer function taking into account the effects of polarization. For simplification, we have neglected the pump depletion.

Thus, the impacts of pump SOP fluctuations on the amplified signal with the presence of PMD are the additional pump to signal RIN transfer, as compared to Ref.13, and a novel noise, the SOP beating noise is transferred to the signal. Two examples of the SOP fluctuations transfer function are plotted in figure 6.1 for co- and counter-pumped configurations. We see that they are all low-pass filter transfer function. For comparison, the traditional RIN transfer functions for the two configurations are also plotted in the figure 6.1. From (6.7), we find the maximum and the bandwidth of the SOP fluctuations transfer function as

$$\left|\underline{H}_{\mathrm{SOP}}(L,0)\right|^2=\frac{2L_dL_{eff}\left(C_RP_{p0}\right)^2}{3}\quad\text{and}\quad \Delta f_H=\frac{1}{\pi}\int_{-\infty}^{+\infty}\frac{\left|\underline{H}_{\mathrm{SOP}}(L,f)\right|^2}{\left|\underline{H}_{\mathrm{SOP}}(L,0)\right|^2}\mathrm{d}f=\frac{1}{2\pi\left|\beta_{sp}\right|L_d} \tag{6.8}$$

In practice, this last one is typically a few hundreds of megahertz for co-pumped Raman amplifiers and a few megahertz for counter-pumped Raman amplifiers. This is to be compared with the traditional RIN transfer[13], where the corner frequencies are typically of order of a few megahertz for co-pumping and a few kilohertz for counter-pumping.

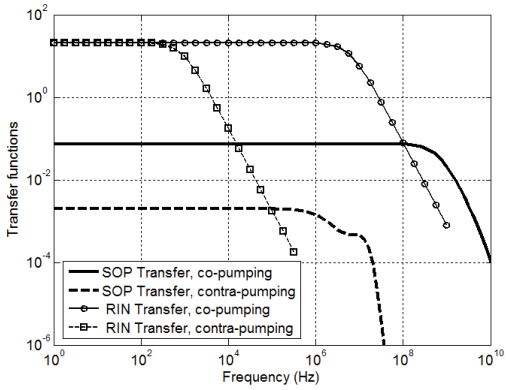

Fig. 6.1 Examples of the transfer functions for co- and counter-pumped configurations .

6.3 Performance degradation estimations

The system performance degradation can be estimated by in terms of the Q penalty[13]. First, it is worth noting that, for the two pumping configurations, we have $\int_{\Re}\left|\underline{h}_{\mathrm{RIN}}(z,f)\right|^2\mathrm{d}f=3\int_{\Re}\left|\underline{H}_{\mathrm{SOP}}(z,f)\right|^2\mathrm{d}f$. Therefore, if the pump RIN is constant in the range of interest and the receiver bandwidth is much larger than Δf_{H}, we see that the acceptable value of pump RIN is reduced by a factor of 4/3, or 1.25 dB, as compared to Ref.13. Moreover, we see clearly from figure 6.1 that the novel RIN transfer function $\left|\underline{H}_{\mathrm{RIN}}(L,f)\right|^2=\left|\underline{h}_{\mathrm{RIN}}(L,f)\right|^2+\left|\underline{H}_{\mathrm{SOP}}(L,f)\right|^2$ implies that, as compared to Ref 13, the spectral range of the transferable RIN is extended by two or three orders of magnitude, for the two configurations. This can result in important impacts on the Q penalty estimation, and, therefore, on the pump RIN requirements. For example, in the counter-pumped configuration, it was found that the pump RIN requirement could be remarkably relaxed by the technique of introducing a high-pass filter before the photoreceiver, whose corner frequency is larger than that of the traditional RIN transfer function [13,34]. However, becoming dominating before the traditional RIN transfer, the additional RIN transfer assisted by PMD should not be omitted in this case.

In order to discuss the impact of beating noise, we assume that the two pump polarization components are statistically independent and their lineshapes can be both considered as Lorentzian, with linewidth $\Delta F_{x,y}$ and central frequencies

shifted by Δf_{xy}. For co- and counter-pumped configurations, figure 6.2 shows two examples of Q penalty as a function of the pump linewidth $\Delta F_c = \Delta F_x + \Delta F_y$ and the frequency shift Δf_{xy}, where the baseline of the quality factor Q_s is chosen to be 10 for both the two configurations. From the figures, we see that the Q penalty decreases always with the frequency shift Δf_{xy}. Therefore, it could be a solution for canceling out the beating noise transfer to separate in spectrum the two field components of the pump, as already mentioned[31]. This should be especially useful for the co-pumped configuration, where the Q penalty is much more important and the Raman pump is frequently the polarization combined diodes[31].

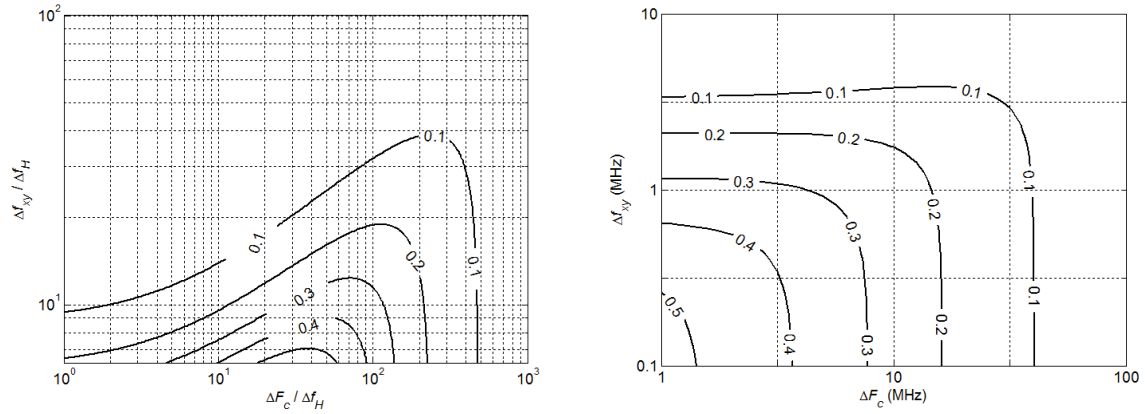

(a) (b)

Fig. 5.2. Two examples of Q penalty as a function of the pump linewidth and the frequency shift for (a) co-pumping and (b) counter-pumping.

7 CONCLUSION

Fundamental limits for the noise figure of gain distribution over a lossy fiber have been discussed by using a simple model for fundamental quantum noise generation. Relation with the standard ASE approach and physical meaning of effective noise have been clarified

We have proposed a novel frequency model to evaluate the pump to signal intensity noise transfer in multi pump amplification of WDM signals. The model takes into account the pump depletion and pump-to-pump, pump-to-signal and signal-to-signal interaction. We have discuss the influence of DBR in terms of system penalty by taking into account its polarization degree with respect to that of the output signal. The DRB crosstalk coefficient, the ASE enhancement factor and the Q penalty have been discussed as a function of the percentage of the forward pumping and the Raman gain.

We also have pointed out that the pump State of Polarization (SOP) temporal fluctuations in the presence of PMD influence the amplified signal noise and propose an analytical expression of the transfer function. Cutoff frequency of PMD assisted noise transfer appears higher from 2 to 3 orders of magnitude than traditional noise transfer. Its influence has been discussed in terms of Q penalty.

References

[1] G.P. Agrawal, Fiber-Optic Communication Systems, 2nd Ed. Wiley InterScience, 1997.

[2] G. P. Agrawal, "Nonlinear Fiber Optics", 3rd ed. San Diego, CA Academic Press, 2000.

[3] E. Desurvire. "Erbium Doped Fiber Amplifiers, Principles and Applications". John Wiley & sons, New-York, 1994.

[4] B.M.Oliver "Thermal and quantum noise". Proc. IEEE, pp 436-454, May, 1965

[5] H.A. Haus, "From classical to quantum noise". J. Opt. Soc. Am. B, 12, 11, 2019-2036, 1995.

[6] R.H. Kingston "Detection of optical and infrared radiation". Springer-Verlag Berlin, 1978

[7] R. C. Steele, G. R. Walker, N. G. Walker, "Sensitivity of optically preamplified receivers with optical filtering".IEEE Photonics Technology Letters 3, 6, pp545-547, June,1991.

[8] P. Gallion "A classical corpuscular approach to optical noise". OSA, Trends in Optics and Photonics (TOPS), Vol XXX : Optical Amplifier and their applications, Edited by Susumu Kinoshita, Jeffrey C. Livas & Gerald van der Hoven, Optical Society of America, pp. 12-35, Washington DC, 1999.

[9] M. Nissov, K. Rottwitt, H.D. Kidorf, and M.X. Ma, "Rayleigh crosstalk in long cascades of distributed unsaturated Raman amplifiers," IEE Electron. Lett. 35, 997-998, 1999.
[10] H. Heffner, "The fundamental noise limit of linear amplifiers", Proc. of the IRE, 1604-1608,1962.
[11] P. Gallion, "Classical phase-amplitude description of optical amplifier noise". Proceedings of SPIE Vol 5260, Applications of Photonic Technology 6 : Closing the gap between theory, development and applications. Edited by Roger A. Lessard and Georges A. Lampropoulos, pp 96-102, SPIE Bellingham WA, 2003.
[12] R.-J. Essiambre, P. J. Winzer, J. Bromage, and C. H. Kim, "Design of bidirectionally pumped fiber amplifiers generating double Rayleigh backscattering," Photon. Technol. Lett., vol. 14, pp. 914–916, 2002.
[13] C. R. S. Fludger, V. Handerek, and R. J. Mears, "Pump to Signal RIN Transfer in Raman Fiber Amplifiers" IEEE, J. Lightwave Technol. 19, pp. 1140–1148, 2001.
[14] S. Jiang and P.Gallion, "Theoretical Analysis on the PMD-assisted pump-to-signal noise transfer in Distributed Fiber Raman Amplifier", IEEE/OSA Journal of Lightwave Technology Volume 25, Issue 10, Oct. 2007.
[15] H.A. Haus, "Quantum circuit theory of phase-sensitive linear systems", IEEE Journal of quantum Electron. QE-23, 2, pp 212-221, 1987
[16] P. Gallion,"Basics of Digital Optical Communications", Undersea Fiber Systems, Edited by J. Chesnoy, pp. 51-93, Academic Press New York, 2002.
[17] B.O. Nilsson, "Noise mechanisms in laser diodes", IEEE Trans. on electron devices, 41, 11, 2139-2150,1994
[18] S. Donati, " Noise in an optical amplifier: Formulation of a new semi classical model", IEEE J. of Qu. Electron., 33, 9, 1481-1488, 1997.
[19] B. Bristiel, S. Jiang, P. Gallion And E. Pincemin, "New Model of Noise Figure and RIN Transfer in Fiber Raman Amplifiers", IEEE Photonics Technol. Lett. PTL, 18-8, pp. 980 - 982, April 2006.
[20] H. Haus (1998), "The noise figure of optical amplifiers", IEEE Photonics Techno, Lett., vol10. no 11, 1602-1604.
[21] D.M. Baney, P. Gallion and R.S. Tucker, "Theory and Measurement Techniques for the Noise Figure of Optical Amplifiers", Optical Fiber Technology 6, 122-154, 2000.
[22] S. Namiki and Y. Emori, "Ultrabroad-band Raman amplifiers pumped and gain-equalized by wavelength-division-multiplexed high-power laser diodes", IEEE J. Select. Topics Quantum Electron., vol. 7, pp.3–16, Jan. 2001.
[23] Junhe Zhou, Jianping Chen, Xinwan Li, Guiling Wu, and Yiping Wang, "A novel frequency domain model to calculate the pump to signal RIN transfer in multi-pump Raman fiber amplifiers" Optics Express vol. 14., No. 23, pp. 11024-11035, 2006.
[24] H. Kidorf, K. Rottwitt, M. Nissov, M. Ma, and E. Rabarijaona, "Pump interactions in a 100-nm bandwidth Raman amplifier", IEEE Photon. Technol. Lett. 11, 530-532, 1999.
[25] S. Jiang, B. Bristiel, Y. Jaouën, P. Gallion and E. Pincemin, "Bit-Error Rate Evaluation of the Distributed Raman Amplifiers Based Transmission Systems with the Double Rayleigh Backscattering Noise", IEEE Photonics Technology Letters , Vol. 19-7, pp.468-470 April 2007.
[26] S. Jiang, B. Bristiel, Y. Jaouen, P. Gallion, E. Pincemin, and S. Capouilliet, "Full characterization of modern transmission fibers for Raman amplified-based communication systems" Optics Express, 15-8, pp. 4883-4892, April 2007.
[27] M. O. van Deventer, "Polarisation properties of Rayleigh backscattering in single-mode fibers," IEEE J. Lightwave Technol. 12, 1895-1899, 1993.
[28] M. Nissov, K. Rottwitt, H.D. Kidorf, and M.X. Ma, "Rayleigh crosstalk in long cascades of distributed unsaturated Raman amplifiers" IEE Electron. Lett. 35, 997-998, 1999.
[29] M. N. Islam and R. W. Lucky, "Raman Amplifiers for telecommunications 2 : Sub-Systems and Systems", Chap. 15, J. Bromage, P. J. Winzer, and R.-J. Essiambre, Springer-Verlag, 2004.
[30] Q. Lin and G. P. Agrawal, "Vector theory of stimulated Raman scattering and its application to fiber-based Raman amplifiers", J. Opt. Soc. Am. B 20, 1616-1631, 2003.
[31] Martinelli, L. Lorcy, A. Durécu-Legrand, D. Mongardien, S. Borne, and D. Bayart, "RIN transfer in copumped Raman Amplifiers using polarization-combined diodes", IEEE Photon. Technol. Lett. 17, 1836-1838, 2005.
[32] A. Galtarossa, L. Palmieri, M. Schiano, and T. Tambosso, "Statistical characterization of fiber random birefringence," Opt. Lett. 25, 1322-1324, 2000.
[33] P. K. A. Wai and C. R. Menyuk, "Polarization mode dispersion, decorrelation and diffusion in optical fibers with randomly varying birefringence", IEEE J. Lightwave Technol. 14, 148-157, 1996.
[34] M. D. Mermelstein, C. Headley, and J.-C. Bouteiller, "RIN transfer analysis in pump depletion regime for Raman fiber amplifiers", Electron. Lett. 28, 403–404, 2002.